



Supplement of

Distribution, chemical, and molecular composition of high and low molecular weight humic-like substances in ambient aerosols

Xingjun Fan et al.

Correspondence to: Xingjun Fan (fanxj@ahstu.edu.cn) and Jianzhong Song (songjzh@gig.ac.cn)

The copyright of individual parts of the supplement might differ from the article licence.

Text S1. Calculation of light absorption and fluorescence parameters.

To characterize the optical and chemical properties of HULIS fractions, several parameters were calculated, including specific UV absorbance at 254 nm ($SUVA_{254}$), the UV absorbance ratio between 250 and 365 nm (E_2/E_3), spectra slope ratios (S_R), the absorption Angstrom exponent (AAE), and mass absorption efficiency (MAE_{365}), fluorescence indices (FI), biological index (BIX), and humification degree (HIX).

$SUVA_{254}$ represents the specific absorption at 254 nm, which is a measure of the aromaticity of organic matters (Fan et al., 2012; Huo et al., 2021). E_2/E_3 is the ratio of absorbance at 250 nm to that at 365 nm and indicates the relative abundance of aromatic structures in aerosol organics (Chen et al., 2016; Fan et al., 2023). S_R is the spectral slope ratio calculated within specific wavelength ranges (275–295 nm and 350–400 nm) and provides information about the size and complexity of the organic matter (Li et al., 2022).

MAE_{365} and AAE (fitted within the wavelength range of 330–400 nm) are used to assess the light absorption efficiency and spectral dependence of the brown carbon (Fan et al., 2023; He et al., 2023; Huo et al., 2021), which were generally calculated using the following equations:

$$MAE_{365} = \frac{A_{365}}{C \cdot l} \times \ln(10) \quad \text{①}$$

$$A_{\lambda} = K \cdot \lambda^{-AAE} \quad \text{②}$$

where A is the absorbance, λ is the wavelength, C is the carbon content of HULIS, and l is the optical length (0.01 m).

The fluorescence index (FI), biological index (BIX), and humification index

(HIX) were calculated based on the EEM of the HULIS fractions. FI is calculated as the ratios of the fluorescence intensity at excitation and emission wavelengths (Ex/Em) of 370/470 nm to that at 370/520 nm (Qin et al., 2018). BIX is calculated as the ratio of the intensity at Ex/Em of 310/380 nm to that at 310/430 nm (Qin et al., 2018). HIX is calculated as the ratio of the intensity at wavelengths of 255/434–480 nm (average of the values on the line between 255/434 and 255/480 nm) to that at 255/300–344 nm (average of the values on the line between 255/300 and 255/344 nm) (Fan et al., 2021). These indices provide insights into the composition and characteristics of the organic matter present in the HULIS fractions, particularly regarding their fluorescence properties and the degree of biological and humic transformation.

Text S2. FTIR analysis

The functional groups in HMW and LMW HULIS were characterized using a Nicolet iS50 FTIR spectrometer (Thermal Fisher, USA). Before analysis, the freeze-dried MW HULIS and pure KBr were thoroughly mixed, finely ground, and pressed into pellets under dry conditions. Then, the FTIR spectra of samples were recorded within the wavenumbers ranging from 4000 to 400 cm^{-1} , with a resolution of 4 cm^{-1} . To ensure accuracy, each spectrum was baseline-corrected using the pure KBr spectrum. Fig. S6 depicts the FTIR spectra of HMW and LMW HULIS in both summer and winter aerosols. In general, both HMW and LMW HULIS present similar absorption peaks, including pronounced peaks at 3434 cm^{-1} (O-H stretching of phenols and carboxylic acids), 1721 cm^{-1} (mainly C=O stretching of carboxylic acids),

1636 cm^{-1} (mainly C=C stretching of aromatic rings and C=O stretching of conjugated carbonyl groups) and 1390 cm^{-1} (O-H deformation and C-O stretching of phenolic groups) were observed (Fan et al., 2020; Fan et al., 2016; Mukherjee et al., 2020; Wang et al., 2021). Additionally, weak peaks at 2929-2980 cm^{-1} and 1045-1281 cm^{-1} , attributed to C-H stretching of aliphatic $-\text{CH}_2$ and $-\text{CH}_3$, and C-O stretching of esters and ethers, respectively, were also observed (Fan et al., 2016; Wang et al., 2021; Zhang et al., 2021). These observations indicate that both HMW and LMW HULIS contain complex multi-component mixtures of compounds, encompassing aliphatic and aromatic species, as well as carboxyl and phenolic functional groups.

As shown in Fig. S6, more intense peaks at 1721 and 1636 cm^{-1} were observed in HULISs in summer aerosols compared to those in winter aerosols. In addition, the peaks at 1045-1281 cm^{-1} in summer HULISs appear to be more complex and overlapping than those in winter HULISs. These findings imply higher abundances of aromatic carboxyl acids and other O-containing groups (i.e., $-\text{OH}$, C=O and C-O) in summer HULISs than in winter ones, possibly attributed to complex oxidation reactions prevailing in summer season (Fan et al., 2020; Qin et al., 2022). This could be partly associated with the enhanced oxidation processes driven by the higher concentration of O_3 in summer (Table S1). Our previous study has proved that the O_3 oxidation of BB BrC lead to the generation of more intense peaks at approximately 1725 cm^{-1} (Fan et al., 2020). Moreover, distinct differences in relative peak intensity between HMW and LMW HULIS fractions were observed. HMW HULIS generally exhibit a stronger band at 1721 cm^{-1} compared to LMW HULIS in both seasonal

aerosols (Fig. S6). This finding suggests that HMW HULIS contain a higher abundance of C=O groups, likely associated with the oxidation of the unsaturated structures with addition of polar functional groups (e.g., -COOH, >C=O) during SOA processes (Fan et al., 2020; Pillar-Little and Guzman, 2018).

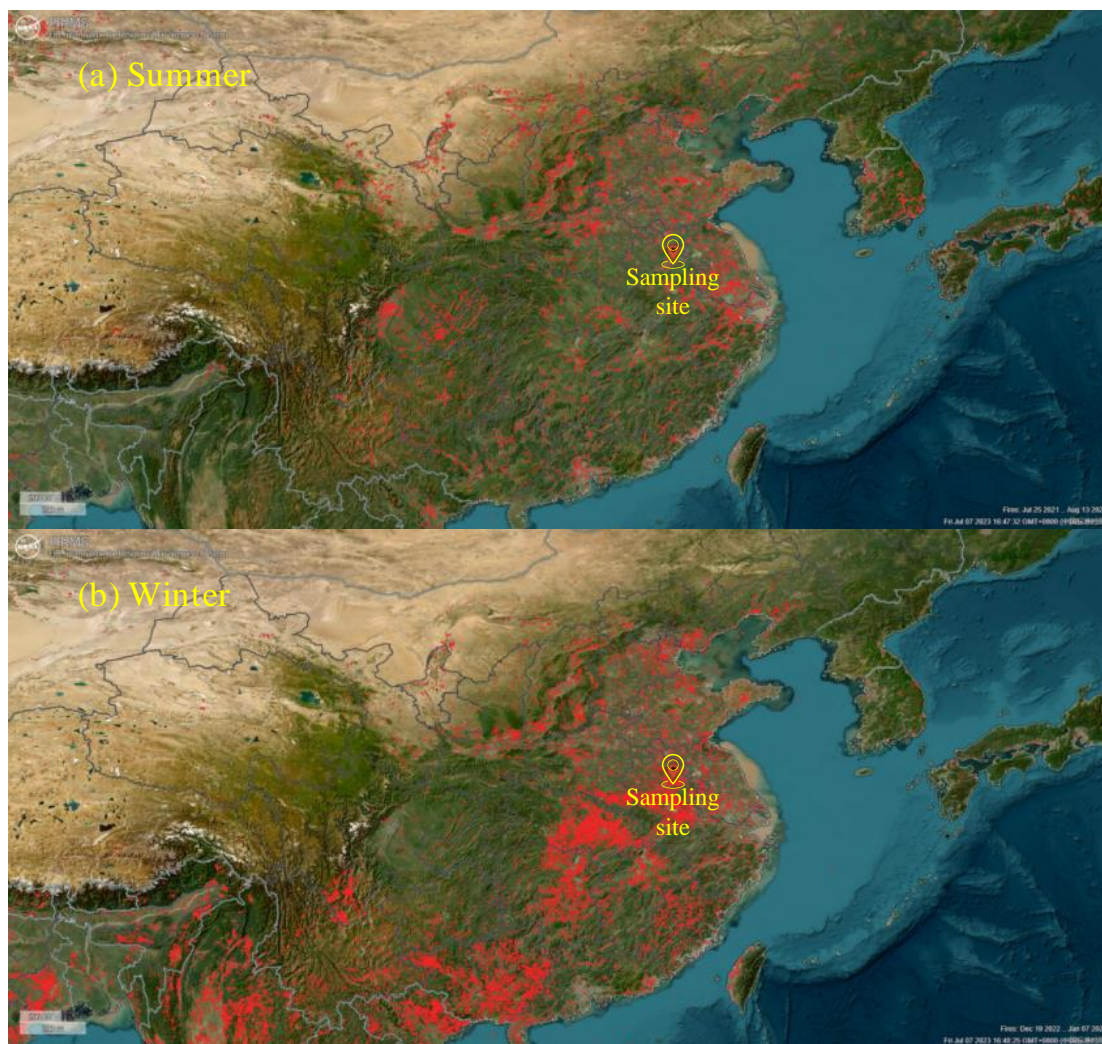


Fig. S1. The distribution of fire spots observed at sampling site during sampling period (<https://firms.modaps.eosdis.nasa.gov/map/>).

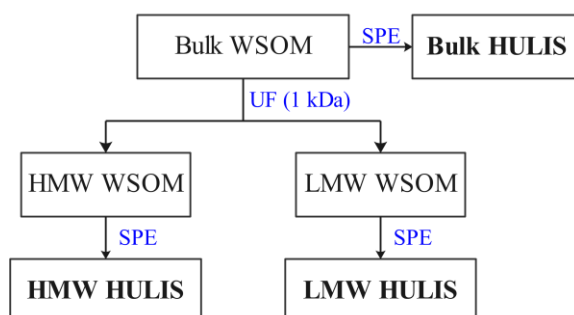


Fig. S2. Separation of size HULIS using ultrafiltration and solid phase extraction.

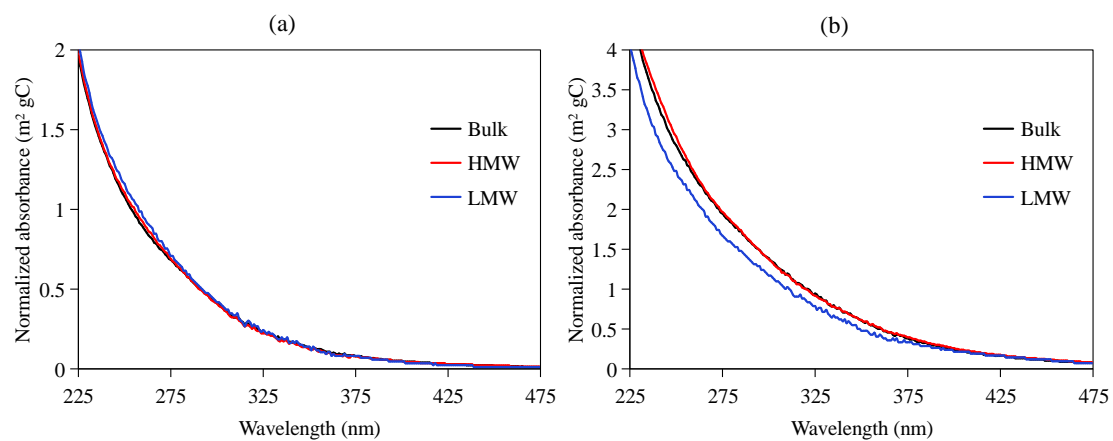


Fig. S3. The normalized UV-vis spectra with TOC of bulk, HMW and LMW HULIS from (a) summer and (b) winter aerosol samples.

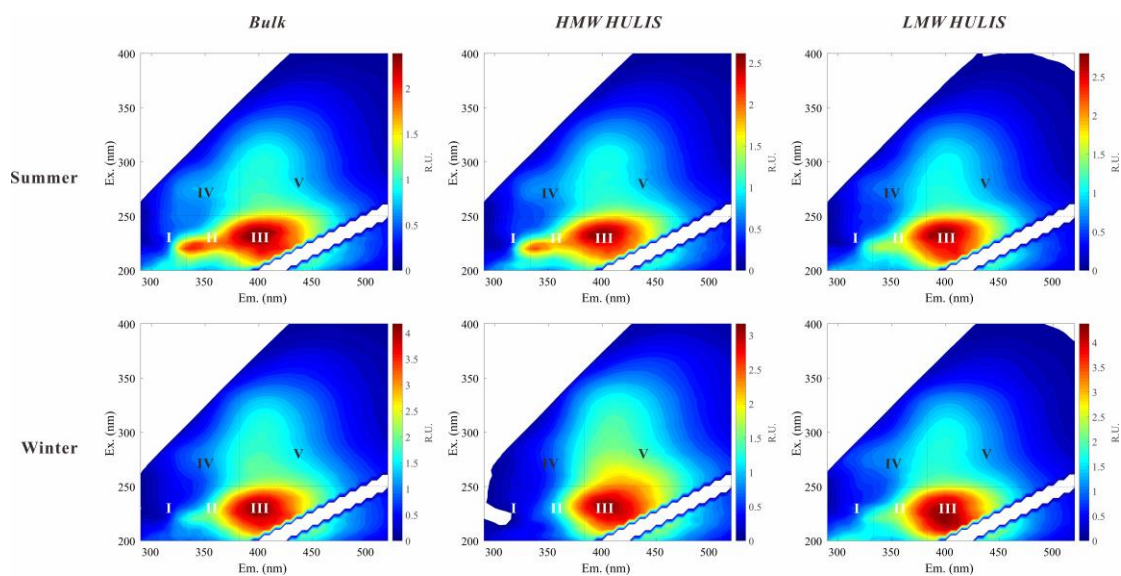


Fig. S4. Representative EEM contours of HMW and LMW HULIS from Bulk and ambient aerosols.

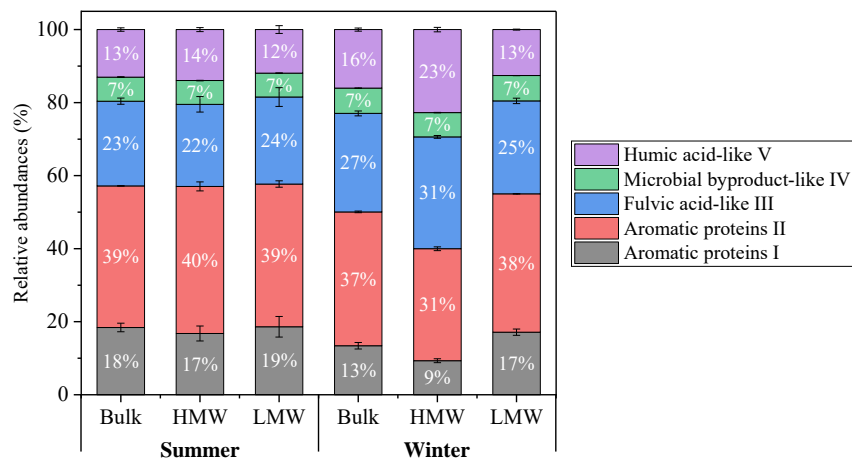


Fig. S5. The distributions of FRI-derived fluorophores within Bulk and MW HULIS fractions in summer and winter aerosols.

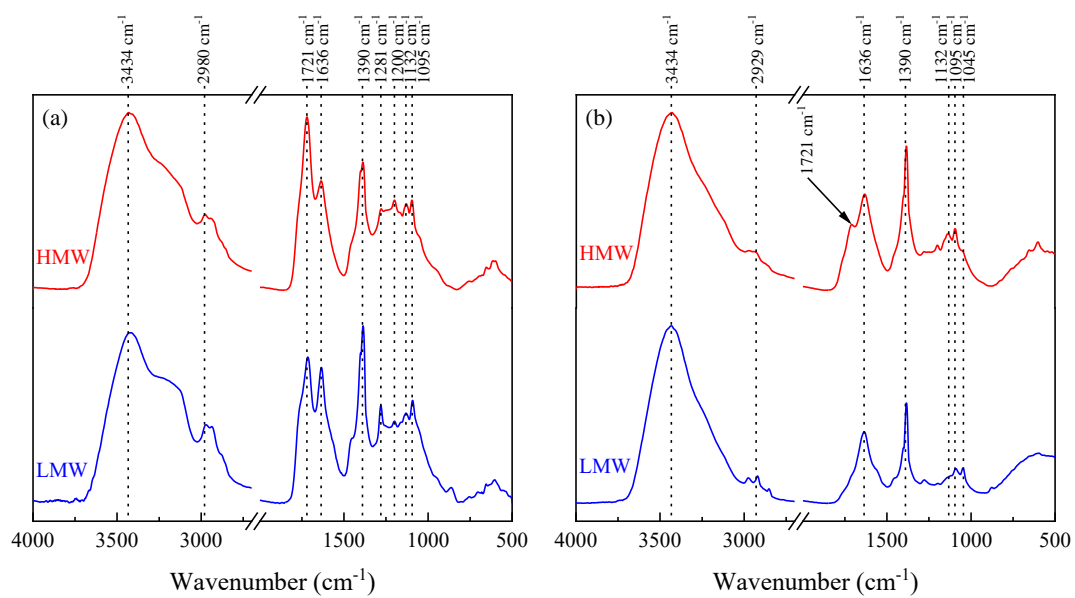


Fig. S6. FTIR spectra of HMW and LMW HULIS in (a) summer and (b) winter aerosols.

Table S1. Concentrations of NO₂, SO₂ and O₃ at the sampling site during summer and winter.

Date	NO ₂ (µg m ⁻³)	SO ₂ (µg m ⁻³)	O ₃ (µg m ⁻³)
<i>Summer</i>			
2021-07-25	7	10	80
2021-07-27	4	8	49
2021-07-29	5	9	73
2021-07-31	9	14	147
2021-08-02	14	14	136
2021-08-04	10	12	96
2021-08-06	12	13	108
2021-08-08	16	13	119
2021-08-10	20	14	178
2021-08-12	13	12	83
Mean	11.0 ± 5.0	11.9 ± 2.2	106.9 ± 38.8
<i>Winter</i>			
2021-12-19	40	13	70
2021-12-21	60	16	90
2021-12-23	57	11	80
2021-12-25	16	4	62
2021-12-27	45	12	63
2021-12-29	42	14	50
2021-12-31	60	18	71
2022-01-02	67	18	70
2022-01-04	45	11	87
2022-01-06	30	8	70
Mean	46.2 ± 15.5	12.5 ± 4.4	71.3 ± 12.0

Table S2. Compound classes identified by elemental ratios (H/C and O/C).

Species	H/C	O/C
Lipids-like	1.5 < H/C ≤ 2.0	0 ≤ O/C ≤ 0.3
Protein/amino sugars	1.5 < H/C ≤ 2.2	0.3 < O/C ≤ 0.67
Carbohydrates	1.5 < H/C ≤ 2.4	0.67 < O/C ≤ 1.2
Unsaturated hydrocarbons	0.7 < H/C ≤ 1.0	0 < O/C < 0.1
Lignins	0.7 < H/C ≤ 1.5	0.1 ≤ O/C < 0.67
Condensed aromatics	0.2 ≤ H/C ≤ 0.7	0 < O/C < 0.67
Tannins	0.5 < H/C ≤ 1.5	0.67 < O/C ≤ 1.2

Table S3. The average values of intensity-weighted molecular weights (MW), elemental ratios, double bond equivalents (DBE), modified aromaticity index (AImod) and carbon oxidation state (OSC) of unique categories of molecular compounds within each MW HULIS fractions.

		Categories of molecular compounds	MW _w	H/C _w	O/C _w	N/C _w	S/C _w	O/N _w	O/S _w	OM/OC _w	DBE _w	DBE/C _w	DBE-O _w	AImod, _w	OSC _w
Summer	HMW HULIS	Lipids-like	311	1.8	0.2	0.1	0.0	1.5	0.0	1.5	3.1	0.2	-0.4	0.1	-1.4
		Protein/amino sugars	255	1.8	0.5	0.1	0.0	2.8	0.4	2.0	2.7	0.3	-2.5	0.0	-0.8
		Carbohydrates	216	1.8	0.9	0.1	0.1	2.3	3.0	2.7	1.8	0.3	-4.3	0.0	0.0
		Unsaturated hydrocarbons	226	0.7	0.1	0.0	0.1	0.0	1.0	1.3	10.0	0.7	9.0	0.7	-0.6
		Lignins	255	1.2	0.4	0.1	0.0	2.0	0.2	1.9	6.0	0.5	1.3	0.5	-0.4
		Condensed aromatics	222	0.6	0.2	0.1	0.1	0.9	0.5	1.7	9.6	0.9	7.0	0.9	-0.1
		Tannins	228	1.2	0.8	0.3	0.1	2.9	2.4	2.7	4.9	0.7	-1.1	0.3	0.5
	LMW HULIS	Lipids-like	467	1.7	0.2	0.0	0.0	5.3	5.3	1.6	4.8	0.2	-1.0	0.0	-1.3
		Protein/amino sugars	344	1.7	0.6	0.0	0.1	0.1	5.3	2.0	3.2	0.2	-4.5	0.0	-0.6
		Carbohydrates	308	1.7	0.8	0.0	0.1	1.2	7.1	2.5	2.7	0.3	-5.6	0.0	-0.1
		Unsaturated hydrocarbons	0	0	0	0	0	0	0	0	0	0	0	0	0
		Lignins	342	1.3	0.5	0.0	0.0	0.4	0.3	1.9	6.5	0.4	-1.8	0.2	-0.2
		Condensed aromatics	192	0.6	0.6	0.0	0.0	0.0	0.3	1.9	7.1	0.9	2.0	0.9	0.6
		Tannins	300	1.2	0.8	0.0	0.0	0.8	1.0	2.2	5.4	0.5	-3.6	0.1	0.4
Winter	HMW HULIS	Lipids-like	314	1.8	0.2	0.1	0.1	1.6	0.2	1.6	3.0	0.2	0.2	0.0	-1.5
		Protein/amino sugars	208	1.8	0.5	0.1	0.0	0.8	0.5	2.0	2.1	0.3	-2.4	0.0	-0.7
		Carbohydrates	215	2.0	0.9	0.1	0.0	1.9	0.0	2.4	1.3	0.2	-5.3	0.0	-0.2
		Unsaturated hydrocarbons	0	0	0	0	0	0	0	0	0	0	0	0	0
		Lignins	222	1.1	0.4	0.2	0.0	1.5	0.1	1.8	6.8	0.7	2.9	0.7	-0.3
		Condensed aromatics	219	0.6	0.3	0.0	0.0	1.3	0.1	1.5	9.6	0.8	6.1	0.8	-0.1

	Tannins	187	1.0	0.8	0.2	0.0	3.0	0.1	2.5	5.1	0.8	-0.1	0.7	0.7
LMW HULIS	Lipids-like	308	1.7	0.2	0.1	0.0	0.9	0.3	1.6	4.5	0.3	1.5	0.1	-1.3
	Protein/amino sugars	282	1.8	0.5	0.0	0.1	0.6	3.6	2.0	2.1	0.2	-3.9	0.0	-0.8
	Carbohydrates	270	1.8	0.8	0.0	0.1	2.6	7.1	2.6	2.0	0.2	-5.2	0.0	-0.2
	Unsaturated hydrocarbons	0	0	0	0	0	0	0	0	0	0	0	0	0
	Lignins	281	1.2	0.5	0.0	0.0	1.1	0.2	1.9	6.4	0.5	0.2	0.3	-0.2
	Condensed aromatics	180	0.6	0.5	0.3	0.0	0.4	0.0	2.0	7.4	1.0	3.7	1.8	0.4
	Tannins	238	1.1	0.8	0.0	0.0	0.4	0.1	2.2	5.3	0.6	-1.9	0.3	0.5

References

- Chen, Q., Miyazaki, Y., Kawamura, K., Matsumoto, K., Coburn, S., Volkamer, R., Iwamoto, Y., Kagami, S., Deng, Y., Ogawa, S., Ramasamy, S., Kato, S., Ida, A., Kajii, Y., Mochida, M., 2016. Characterization of Chromophoric Water-Soluble Organic Matter in Urban, Forest, and Marine Aerosols by HR-ToF-AMS Analysis and Excitation-Emission Matrix Spectroscopy. *Environ. Sci. Technol.* 50, 10351-10360.
- Fan, X., Cai, F., Xu, C., Yu, X., Wang, Y., Xiao, X., Ji, W., Cao, T., Song, J., Peng, P., 2021. Molecular weight-dependent abundance, absorption, and fluorescence characteristics of water-soluble organic matter in atmospheric aerosols. *Atmos. Environ.* 247.
- Fan, X., Cao, T., Yu, X., Wang, Y., Xiao, X., Li, F., Xie, Y., Ji, W., Song, J., Peng, P., 2020. The evolutionary behavior of chromophoric brown carbon during ozone aging of fine particles from biomass burning. *Atmos. Chem. Phys.* 20, 4593-4605.
- Fan, X., Cheng, A., Chen, D., Cao, T., Ji, W., Song, J., Peng, P., 2023. Investigating the molecular weight distribution of atmospheric water-soluble brown carbon using high-performance size exclusion chromatography coupled with diode array and fluorescence detectors. *Chemosphere* 338, 139517.
- Fan, X., Wei, S., Zhu, M., Song, J., Peng, P., 2016. Comprehensive characterization of humic-like substances in smoke PM_{2.5} emitted from the combustion of biomass materials and fossil fuels. *Atmos. Chem. Phys.* 16, 13321-13340.
- Fan, X.J., Song, J.Z., Peng, P.A., 2012. Comparison of isolation and quantification methods to measure humic-like substances (HULIS) in atmospheric particles. *Atmos. Environ.* 60, 366-374.
- He, T., Wu, Y., Wang, D., Cai, J., Song, J., Yu, Z., Zeng, X., Peng, P., 2023. Molecular compositions and optical properties of water-soluble brown carbon during the autumn and winter in Guangzhou, China. *Atmos. Environ.* 296, 119573.
- Huo, Y., Wang, Y., Qi, W., Jiang, M., Li, M., 2021. Comprehensive characterizations of HULIS in fresh and secondary emissions of crop straw burning. *Atmos. Environ.* 248, 118220.
- Li, X., Yu, F., Cao, J., Fu, P., Hua, X., Chen, Q., Li, J., Guan, D., Tripathee, L., Chen, Q., Wang, Y., 2022. Chromophoric dissolved organic carbon cycle and its molecular compositions and optical properties in precipitation in the Guanzhong basin, China. *Sci. Total Environ.* 814, 152775.
- Mukherjee, A., Dey, S., Rana, A., Jia, S., Banerjee, S., Sarkar, S., 2020. Sources and atmospheric processing of brown carbon and HULIS in the Indo-Gangetic Plain: Insights from compositional analysis. *Environmental Pollution* 267, 115440.
- Pillar-Little, E.A., Guzman, M.I., 2018. An Overview of Dynamic Heterogeneous Oxidations in the Troposphere. *Environments* 5, 104.
- Qin, J., Zhang, L., Qin, Y., Shi, S., Li, J., Gao, Y., Tan, J., Wang, X., 2022. pH-Dependent Chemical Transformations of Humic-Like Substances and Further Cognitions Revealed by Optical Methods. *Environ. Sci. Technol.* 56, 7578-7587.
- Qin, J., Zhang, L., Zhou, X., Duan, J., Mu, S., Xiao, K., Hu, J., Tan, J., 2018. Fluorescence fingerprinting properties for exploring water-soluble organic compounds in PM_{2.5} in an industrial city of northwest China. *Atmos. Environ.* 184, 203-211.
- Wang, X., Qin, Y., Qin, J., Long, X., Qi, T., Chen, R., Xiao, K., Tan, J., 2021. Spectroscopic insight into

the pH-dependent interactions between atmospheric heavy metals (Cu and Zn) and water-soluble organic compounds in PM_{2.5}. *Sci. Total Environ.* 767, 145261.

Zhang, T., Shen, Z., Zeng, Y., Cheng, C., Wang, D., Zhang, Q., Lei, Y., Zhang, Y., Sun, J., Xu, H., Ho, S.S.H., Cao, J., 2021. Light absorption properties and molecular profiles of HULIS in PM_{2.5} emitted from biomass burning in traditional "Heated Kang" in Northwest China. *Sci. Total Environ.* 776, 146014.